Acta Astronautica 195 (2022) 243–250

Contents lists available at ScienceDirect

Acta Astronautica

journal homepage: www.elsevier.com/locate/actaastro

Research Paper

A numerical model of dust particle impacts during a cometary encounter with application to ESA's Comet Interceptor mission

Nico Haslebacher [a,*], Selina-Barbara Gerig [a], Nicolas Thomas [a], Raphael Marschall [b], Vladimir Zakharov [c], Cecilia Tubiana [c,d]

[a] Physikalisches Institut, University of Bern, Bern, Switzerland
[b] Southwest Research Institute, Boulder CO, USA
[c] INAF - IAPS, Roma, Italy
[d] Max Planck Institute for Solar System Research, Göttingen, Germany

ARTICLE INFO

Keywords:
Dust hazard
Comet Interceptor
Numerical model

ABSTRACT

The attitude perturbations caused by large dust particle impacts on a three-axis stabilized spacecraft during a high velocity encounter with a comet are studied. Specifically, a numerical model is used to make order of magnitude estimations in relation to the European Space Agency's Comet Interceptor mission and help constrain requirements for guidance, navigation and control (GNC). Our model is able to reproduce the measurements acquired by the spin-stabilized Giotto spacecraft during its encounter with comet 1P/Halley in 1986. For realistic scenarios the total change in angular velocity that needs to be corrected can reach 1–10 °/s. At closest approach the median shift of the target object on the Comet Camera (CoCa) detector is typically larger then 10 pixels for the modelled scenarios. Our model shows that the encounter velocity, the spacecraft radius and the attitude control rate are the most critical factors. For the free parameters scaling laws are derived.

1. Introduction

All the comets encountered in previous cometary missions (e.g. Giotto, Stardust, and Rosetta) were short period comets (period < 200 years). Short period comets have passed through perihelion many times and thus have been altered by many physical processes arising from passage into the inner Solar System.

Comet Interceptor is a new type of space mission. It is being developed by the European Space Agency (ESA) with the goal of intercepting a long period comet (LPC), preferably one which is dynamically new, or an interstellar object [1]. It is the first mission that will be launched before its primary target has been found. The spacecraft will be launched towards the Sun–Earth Lagrange Point L2 together with ESA's ARIEL mission. Comet Interceptor can wait at L2 for up to three years until a suitable target is found. Potential back-up targets have been described by Schwamb et al. [2]. This new approach is enabled by advance in large sky surveys such as Pan-STARRS and ATLAS and the next generation of sky surveys such as the Vera Rubin Observatory's Legacy Survey of Space and Time (LSST). These sky surveys allow us to detect long period comets (LPCs) inbound at larger heliocentric distances which give us longer warning times of their arrival in the inner Solar System.

However, because the target object is unknown, this approach comes with new challenges during the design-phase of the spacecraft. The spacecraft and its instruments need to be designed to be as flexible as possible to be able to handle a wide range of targets, encounter geometries and potentially hazardous environments [1].

Here we focus on the dangers to attitude control arising from dust particle impacts. The potential issues can be appreciated from consideration of the results from ESA's Giotto spacecraft. The Giotto spacecraft passed comet 1P/Halley at a distance of 596 km on 13 March 1986 [3]. During the approach to the nucleus Giotto was repeatedly hit by dust particles that were large enough to cause attitude perturbations [4]. The total change of Giotto's velocity was 23 cm s^{-1}, which corresponds to a total mass of 0.32 g impacting the spacecraft [5]. At 7.6 s before closest approach the impact of a large particle shifted the angular momentum vector by more than 1° causing Giotto to lose the telecommunications link to earth.

To illustrate further the importance of this question we can discuss the imaging system on Comet Interceptor which is Comet Camera (CoCa). CoCa has a field of view (FOV) of 0.69° × 0.92°. The size on the detector of the nucleus of a comet of 10 km diameter at closest approach (~1000 km) is 0.57°. Thus, attitude perturbations of about

* Corresponding author.
E-mail address: nico.haslebacher@unibe.ch (N. Haslebacher).

https://doi.org/10.1016/j.actaastro.2022.02.023
Received 10 September 2021; Received in revised form 21 February 2022; Accepted 23 February 2022
Available online 12 March 2022

1° would shift the nucleus out of the FOV. To optimize the time that the nucleus is in the FOV an algorithm using sequential convex programming has been published by Preda et al. [6]. In their work they are already considering the possibility large dust particle impacts.

The dust particles will impact the spacecraft at velocities larger then 10 km/s and thus the impacts occur in the regime of hypervelocity impacts and have to be treated as such. Apart from the dust impacts during cometary flyby missions hypervelocity impacts also occur commonly due to space debris. To improve the effectiveness of spacecraft shielding the problem of hypervelocity impact has been studied extensively in the recent years (e.g. [7]; [8]; [9]).

A large fraction of the dust impacts occur during the time interval between 50 s before and after closest approach [5]. The same time interval is also of utmost importance for the acquisition of images not only because the best resolution is achieved at closest approach, but also because during this time the nucleus can be observed over a large range of phase angles giving the most significant photometric measurements of the nucleus.

This work further explores the issue of potential attitude perturbations caused by dust impacts by modelling different encounter scenarios numerically. The goal of the work is to make predictions of the attitude perturbations dust impacts will cause during the encounter for a wide range of parameters to help constrain requirements on the spacecrafts guidance, navigation and control (GNC) in order to keep the nucleus in the field of view of CoCa.

2. Methods

Comet Interceptor is at an early stage in its design. Hence, we adopt a general approach that might also be useful for future missions of this type.

Because there is only limited knowledge about the spacecraft design and the target object the modelling is approached by making reasonable assumptions and using unknowns as free input parameters. In this section the assumptions and parameters are explained. We use the following approximations:

- Homogeneous mass distribution and cylindrical shape of the spacecraft
- Force-free radial outflow of the cometary dust
- Particle size bins that follow a power law size distribution
- Poisson distribution for the number of dust impacts in a given time
- The absolute dust particle velocity in the momentum transfer equations has been neglected
- Idealized attitude control system.

Without the knowledge of the specific spacecraft design we need to make an educated guess about the moments of inertia of the spacecraft. For the sake of simplicity it is assumed that the spacecraft has a homogeneous mass distribution. Further, the shape of the spacecraft is approximated by a cylinder. Therefore the first and second principal moments of inertia are given by $I_1 = I_2 = \frac{1}{12} M(3R^2 + H^2)$, where M is the mass, R is the radius and H is the height of the spacecraft. The third principal moment of inertia is $I_3 = \frac{1}{2} M R^2$. A homogeneous Giotto-sized cylinder would have moments of inertia of $I_1 = I_2 = 183.5\ \mathrm{kg\,m^2}$, $I_3 = 249.4\ \mathrm{kg\,m^2}$. For comparison, the moments of inertia of Giotto at the encounter were $I_1 = 201.9\ \mathrm{kg\,m^2}$, $I_2 = 210.9\ \mathrm{kg\,m^2}$, $I_3 = 241.3\ \mathrm{kg\,m^2}$ [10].

The local dust density around the nucleus is calculated by approximating the nucleus as a point source and assuming force-free radial outflow. Observations by the Halley Multicolour Camera (HMC) onboard Giotto showed that the azimuthal average (azimuthally integrated dust reflectance multiplied by the impact parameter) is approaching a constant value for distances larger than 60 km, which was equal to about 11 nucleus radii [11]. If the azimuthal average is constant the dust velocity can be assumed to be constant, implying a force-free radial outflow. Similar results have been found for comet 67P/Churyumov–Gerasimenko, the Rosetta target comet [12]. The expression for the local dust density is derived from the equation for force-free radial outflow (see e.g. [13] for an introduction to this)

$$\rho_d(\Delta) = \frac{Q_d}{4\pi\Delta^2 v_d}, \tag{1}$$

where Δ is the distance to the point source, Q_d is the dust production rate and v_d is the outflow velocity averaged over all particle masses.

The dust mass distribution is modelled by using logarithmic particle mass bins and assuming that the particles follow a power law distribution. The power law takes the form $n_d(>m) = k \cdot m^{-\alpha}$, where $n_d(>m)$ is the cumulative mass dependent number density with m being the particle mass, α is the cumulative power law index and k is a constant that is used to normalize the mass dependent dust density to the bulk dust density calculated with Eq. (1). The cumulative power law index measured at 1P/Halley is $\alpha = 0.88$ for $10^{-9}kg \geq m \geq 10^{-13}kg$ and $\alpha = 0.55$ for $m \geq 10^{-9}$ by [14,15], which was derived from a power law fit to measurements by DIDSY and PIA [16]. We chose to constrain the range of the dust particles with a lower cutoff $m_{min} = 10^{-13}kg$, because the contribution of smaller particles to the total mass and the total momentum transfer is negligible (e.g. [15] Figure 10) and the chosen power law index is not valid for smaller particles. The higher mass cutoff, m_{max}, is chosen such that

$$4\pi\Delta^2 v_d \cdot \sum_{m=m_{min}}^{m_{max}} n_d(m) m = Q_d, \tag{2}$$

where $n_d(m)$ is the mass dependent number density, which is based on [15] Figure 10 and $4\pi\Delta^2$ is the surface area of the sphere enclosing the nucleus at a distance of $\Delta = 600$ km. Because the bulk dust velocity is averaged over all particle masses and heavier particles have lower velocities the bulk dust velocity is dependent on the higher mass cutoff. Therefore, the higher mass cutoff needs to be determined by iteration. The resulting higher mass cutoff is $m_{max} = 10^{1.4}$ kg ≈ 0.04 kg. For this model we use ten particle mass bins per decade.

The dust particle impacts are treated as a Poisson process. The Poisson distribution is given by

$$P(x) = e^{-\lambda} \cdot \frac{\lambda^x}{x!}. \tag{3}$$

In our case, $P(x)$ is the probability that there are x dust impacts in a given time and λ is the expected number of impacts in this given time. The position of impact on the shield is drawn from a uniform probability distribution. Due to the random nature of the dust particle impacts we are running the simulation for many iterations in order to make probabilistic statements. If not explicitly stated otherwise, we use 1000 iterations per scenario.

The velocity of individual large dust particles ejected from comet 1P/Halley were estimated to be in the range of 22–45 m s^{-1} for a dust particle with a mass of 1.4 mg and 5.5–11 m s^{-1} for a dust particle with a mass of 14 mg [17]. Compared to the expected encounter velocity for Comet Interceptor in the range of 10–80 km/s [1] the velocity of the dust particles is negligible. The velocity of the dust particle is therefore ignored for the calculation of the momentum transfer.

For simplicity the modelled attitude control system is idealized, which means that it is able to return the spacecraft to the original attitude instantaneously. In addition, the angular velocity of the spacecraft is reset to zero each time the attitude control system acts. We currently have no knowledge of the implementation of the GNC and we consider this to be a best case. This approach is not a realistic representation of an actual attitude control system, but it allows us to study on which time-scale the attitude control system should act.

The unknowns can be reduced to the following parameters that are used as inputs to the numerical simulation:

- mass of the spacecraft, M
- radius of the spacecraft, R

- height of the spacecraft, H
- dust production rate, Q_d
- relative velocity at encounter, v
- distance to nucleus at closest approach, Δ_{CA}
- time interval between attitude corrections, ΔT

These input parameters create a parameter space where all the parameters, except frontal area and height of the spacecraft, are linearly independent. Thanks to the linear independence, the parameters can be studied separately from each other. The changes in velocity and angular velocity have a inverse linear relationship with the spacecraft mass at the time of the encounter. The radius of the spacecraft is needed to calculate the frontal area $A = \pi R^2$, which describes the cross-section for collisions with the dust particles. The dust production rate describes how active the object is. After the dust particles leave the surface of the nucleus, they get accelerated by the outflowing gas because of the drag force. To estimate the dust outflow velocity as a function of the dust production rate a separate insulation driven model is used.

We generate our simulation results using the simulation pipeline first described in [18] and used in several publications thereafter [12, 19–22]. In the simulations the gas flow is calculated with a DSMC (Direct Simulation Monte Carlo) code in 3D around a spherical nucleus of radius $R_N = 2$ km out to a spherical boundary of 10 km from the nucleus centre. The calculations for the gas field become expensive in terms of computational power when increasing the production rate and we therefore limit our maximum simulated gas production rate to $Q_g = 200$ kg/s. The dust-to-gas ratio is assumed to be 1. The dust particle dynamics is calculated in a second step by taking into account forces of gas drag (F_D) and nucleus gravity (F_G) through application of an equation of motion of the form:

$$m_d \cdot \vec{a} = m_d \vec{g_x} + \frac{1}{2} C_D m_g n_g \pi r_d^2 |\vec{V_g} - \vec{V_d}|(\vec{V_g} - \vec{V_d}), \tag{4}$$

with m_d and r_d being the dust particle mass and radius and $\vec{a}$ is the dust acceleration. m_g and n_g are the gas molecular mass and number density and $(\vec{V_g} - \vec{V_d})$ is the relative velocity of the dust particle to the gas flow [23]. We only considered H_2O outgassing in our simulations. C_D is the drag coefficient calculated using the relation given in [24] and $\vec{g_x}$ is the local gravitational acceleration. To calculate the gravitational acceleration we assumed a bulk density of 537.8 kg/m^3 [25] corresponding to the bulk density of comet 67P/Churyumov–Gerasimenko measured during the Rosetta mission. Our simulated dust particles in the size range between 10 nm and 1 dm are spherical and have a similar density of 533 kg/m^3. In the sub-solar direction the gas drag force dominates dust particle motion in the coma up to a certain size limit dependent on the production rate. Particles for which the drag force cannot overcome gravity are not lifted from the surface. The final dust velocities for each particle size are then acquired by averaging the velocities in all simulation cells between 9 and 10 km nucleus-centric distance in a 30° cone around the sub-solar direction. In our analysis, we used results from five simulated particle size bins per size decade.

The velocity of dust particles as a function of their radius is approximated by a power law fit of the form $v_d(m) \approx k \cdot m^{-q}$. The corresponding fitting parameters are listed in Table 1. From these basic power law relationships, we can estimate a dust velocity for an arbitrary particle in our predefined range of $10^{-13} - 0.04$ kg. To estimate a dust velocity for higher dust production rates the velocities are extrapolated with a power law fit of the form $v_d(Q_d, m) = a(m) \cdot {Q_d}^{b(m)}$, where $v_d(Q_d, m)$ is the dust velocity of a given dust mass and $a(m)$ and $b(m)$ are the fitting parameters. The bulk dust velocity is then estimated by averaging the mass dependent dust velocities over all the mass bins by using the total mass of each mass bin as weighting. This allows us to define v_d in Eq. (1).

The encounter velocity describes the velocity of the spacecraft in the reference frame of the comet. Looking at it from the reference frame of the spacecraft, the encounter velocity is equivalent to the impact velocity of the dust particles, because the velocity of individual dust particles is neglected.

Table 1
Power law fitting parameters for the mass dependent dust velocities. The power law has the form $v_d(m) \approx k \cdot m^{-q}$.

Production rate	2 kg/s	20 kg/s	200 kg/s
q	0.169	0.164	0.154
k	0.082	0.268	0.910

In terms of dust hazard the encounter geometry is spherically symmetric, because a point source approximation is used. Therefore, the only parameter needed to describe the trajectory of the spacecraft is the distance to the nucleus at closest approach Δ_{CA}.

Because of our simplified modelling approach we get only one input parameter in relation to the attitude control system. The input parameter is the time interval in between the instantaneous corrections of the attitude control system.

3. Theory/calculation

The relation of the change in velocity Δv of the spacecraft with a mass M to the total mass of dust m_0 impacting the spacecraft at a velocity v_0 is given by momentum conservation

$$m_0 v_0 = \Delta v M - m_r v_r, \tag{5}$$

where m_r and v_r are the mass and velocity of the ejected particles. This equation implicitly assumes that velocities of the impact and ejected particles lie along the same line. This assumption is justified by the fact that due to symmetry reasons the momentum transfer in other directions is cancelling itself out as illustrated by . Using Eq. (5), Δv can be related to m_0 as

$$\Delta v = \frac{m_0 v_0}{M}\left(1 + \frac{m_r v_r}{m_0 v_0}\right) = \frac{m_0 v_0}{M}(1 + \epsilon), \tag{6}$$

where the momentum enhancement factor $\epsilon = \frac{m_r v_r}{m_0 v_0}$ is introduced to describe the increase in momentum transfer due to hypervelocity impact processes such as cratering [5]. The momentum enhancement factor is depended on the impact velocity. We fit the momentum enhancement factor by

$$\epsilon = 0.144 \cdot \frac{(v_0 - 0.55)^2}{v_0}, \tag{7}$$

where v_0 is the impact velocity in [km s^{-1}] [26]. The change in angular velocity caused by a single dust impact is

$$\Delta\omega_i = (1 + \epsilon)\frac{m_d \cdot v \cdot a_i}{I_i}, \tag{8}$$

where m_d is the mass of the dust particle and a_i are the projections of the impact position on the x- and y-axis. The x- and y-axis are defined perpendicular to the movement direction. Explicitly this can be written as $a_1 = a \cdot \sin(\phi)$ and $a_2 = a \cdot \cos(\phi)$, where a is the distance of the impact position to the z-axis and ϕ is the angle between the x-axis and the impact position. The total change in angular momentum is $\Delta\omega = \sqrt{\Delta\omega_1^2 + \Delta\omega_2^2}$.

For spin-axis stabilized spacecraft such as Giotto, dust impacts produce nutation. The magnitude of the nutation can be quantified by the nutation angle θ which is defined by $\tan\theta = \frac{\Delta L_T}{L_3}$, where ΔL_T is the total change in transverse angular momentum and L_3 is the third component of the angular momentum $\vec{L}$. The total change of transverse angular momentum is $\Delta L_T = \sqrt{\Delta L_1^2 + \Delta L_2^2}$ with $\Delta L_i = (1+\epsilon) \cdot a_i \cdot v \cdot m_d$. To compare the simulated change in angular velocity $\Delta\omega$ with the nutation angle measured by Giotto an equivalent formulation which states $\Delta L_i = I_i \cdot \Delta\omega_i$ can be used.

For the sake of simplicity it is assumed that there is no initial nutation ($L_{1,0} = L_{2,0} = 0$). Thus, the initial angular momentum of the

Table 2
Comparison of our model with measurements taken by Giotto. The measured Δv of Giotto is taken from [27]. The measured nutation angles are taken from [4] (Fig. 1). The following input parameters are taken from [28] and [29]: $\Delta T = \infty$, $M = 573.7$ kg, $Q_d = 30000$ kg/s, $H = 1.1$ m, $\Delta_{CA} = 596$ km, $v = 68.373$ km/s, $R = 0.93$ m.

Percentile	Total Δv [cm s^{-1}]	Nutation angle att = −200 s [°]	Nutation angle att = −50 s [°]
25th	7.15	0.0003	0.0052
50th (Median)	18.61	0.0010	0.0192
75th	57.79	0.0047	0.1025
95th	650.61	0.0854	2.3852
Measurement data	23.2	∼ 0.03	∼ 0.07

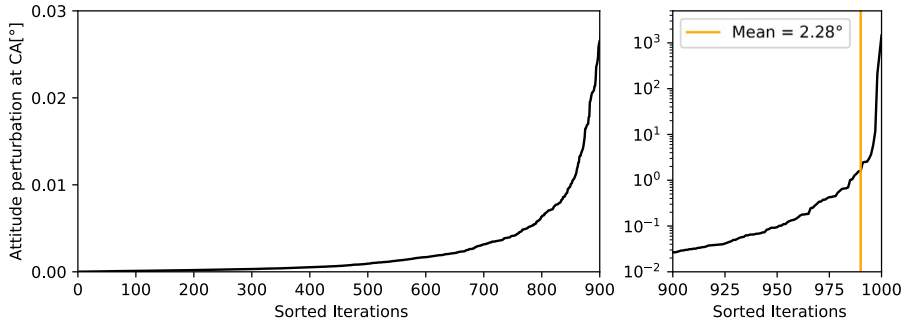

Fig. 1. The attitude perturbation at closest approach of each iteration are sorted from smallest to largest. The figure on the right shows the steep increase between the sorted iterations 900–1000 on a logarithmic scale. The input parameters are set as $\Delta T = 1$ s, $M = 500$ kg, $Q_d = 30000$ kg/s, $H = 1.5$ m, $\Delta_{CA} = 1000$ km, $v = 60$ km/s, $R = 1$ m.

Giotto spacecraft is $|\vec{L}_{initial}| = L_0 = L_3 = I_3 \cdot \omega_{3,0}$ with $\omega_{3,0} = \frac{2\pi}{T_{3,0}}$ where $T_{3,0}$ is the initial spin period of the spacecraft. Hence, the initial spin period of the spacecraft is required as an additional input parameter for the modelling of Giotto.

4. Results

4.1. Validation with the Giotto results

To validate we chose to apply our model to the Giotto mission and compare it to measurements acquired during the encounter with comet 1P/Halley. The model of the encounter of Giotto with comet 1P/Halley is different in only one aspect compared to the model used for Comet Interceptor, which is that the spin-axis stabilization of Giotto is taken into account when calculating the attitude perturbations. For this comparison we use both the total change in angular velocity and the nutation angle at 200 and 50 s before closest approach, which are listed in Table 2.

Due to the random nature of the dust particle impacts it is important to understand the probabilities associated with the attitude perturbations. To show this the iterations were sorted by the attitude perturbation at closest approach in Fig. 1. In the specific simulation case shown in Fig. 1 the expected value of the attitude perturbation which is described by the mean is in the 99th percentile. Hence the mean value provides a poor representation of the data-set as a whole whereas percentile ranges provide a better representation.

4.2. Comet interceptor calculations

Here we are modelling the attitude perturbations for Comet Interceptor with a focus on the shifts these perturbations cause on the detector of CoCa. The telescope of CoCa is a heritage of the CaSSIS telescope (e.g. Thomas et al. 30) with a focal length of 875 mm and an aperture of 13.5 cm. The detector size is 1504 × 2000 pixels with a pixel scale of 8 μrad.

In Fig. 2, we compare the attitude perturbations of a single iteration to the median over all the iterations. The discrete nature of the dust particle impacts is demonstrated in Fig. 2(a). Further, we show that large dust particle impacts can happen tens of seconds before closest approach. In Fig. 2(b) the median of each time point taken over all the iterations is shown. The saw-tooth shape is visualizing how the idealized GNC acts.

Table 3
Percentiles for the number of impacts per particle mass decade. The relevant input parameters are set as $Q_d = 30000$ kg/s, $\Delta_{CA} = 1000$ km, $R = 1$ m.

Percentile	Expected number of impacts per particle mass				
	1 g	100 mg	10 mg	1 mg	100 µg
99th	1	2	6	13	40
90th	0	1	3	9	27
75th	0	0	0	5	21
50th	0	0	0	4	16

Table 4
Exponents b fitted to the medians based on a power law of the form $f(x) = a \cdot x^b$ using a least-squares fit as seen in Fig. 4.

Parameter	Q_d	v	ΔT	R
Scaling law exponent b	0.82	3.61	2.85	3.63

In Fig. 3 the attitude perturbations during the approach without any attitude control are shown. We demonstrate that there is a net change in the angular momentum of the spacecraft. In other words, the angular momentum transfers of all the dust particle impacts are not cancelling each other out, but there is a type of random walk occurring. This shows that the momentum transfer to the spacecraft is dominated by discrete impact events. The nucleus is shifted out of the FOV of CoCa at $50.5\,^{+48.9}_{-30.0}$ seconds (median ± 25th and 75th percentile) before closest approach.

The model can also be used to calculate how many particles of a certain mass impact the spacecraft. In Table 3 the percentiles of the number of impacts per decade are shown for particle masses from 10^{-7} kg to 10^{-3} kg.

In Fig. 4 we show how the input parameters affect the resulting attitude perturbations. The exponents of the trendlines, which are listed in Table 4, give insight into the importance of a parameter. The effects of the spacecraft height is shown in combination with the spacecraft radius in Fig. 5. There are two input parameters that are not studied in further detail, because their relation to the attitude perturbations is apparent from the basic equations. They are the spacecraft mass M and the distance at closest approach Δ_{CA}. Because of the assumption

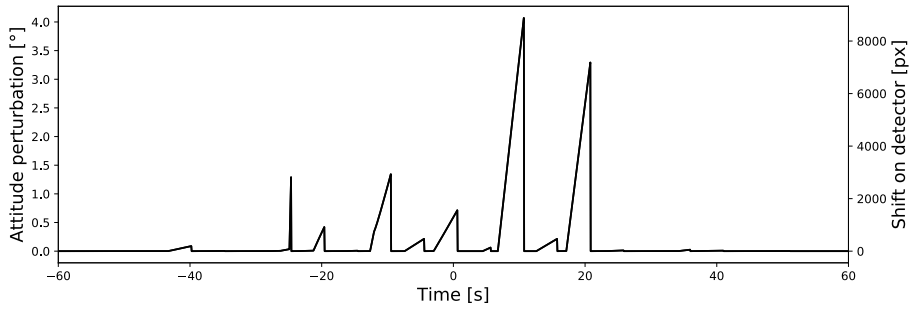

(a) Example of the attitude perturbations of a single iteration.

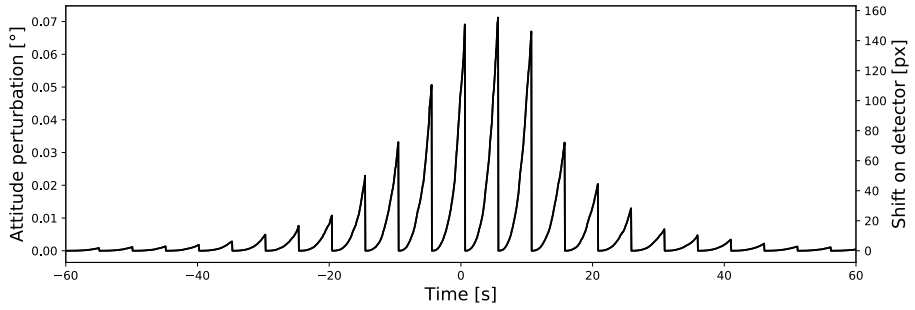

(b) Median attitude perturbations

Fig. 2. The input parameters are set as $\Delta T = 5$ s, $M = 500$ kg, $Q_d = 30000$ kg/s, $H = 1.5$ m, $\Delta_{CA} = 100$ km, $v = 60$ km/s, $R = 1$ m.

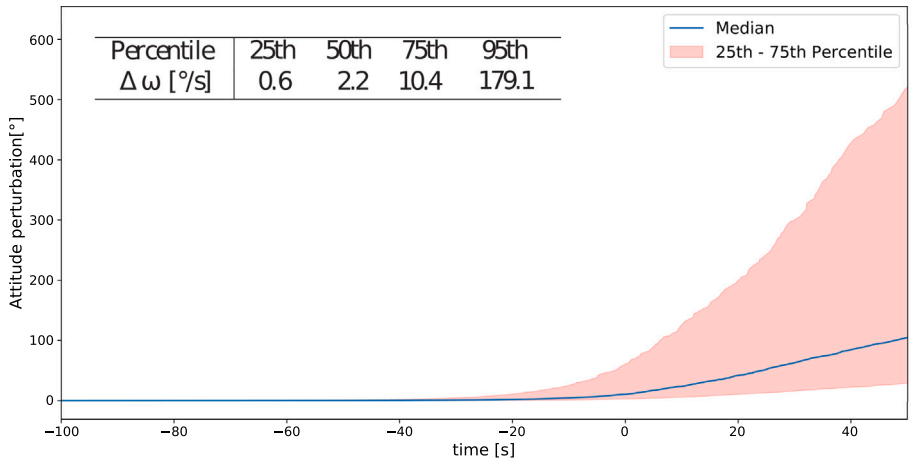

Fig. 3. Expected attitude perturbations without attitude control. The table shows the total change in the angular velocity of the spacecraft during the encounter. The input parameters are set as $\Delta T = \infty$, $M = 500$ kg, $Q_d = 30000$ kg/s, $H = 1.5$ m, $\Delta_{CA} = 1000$ km, $v = 60$ km/s, $R = 1$ m.

of a homogeneous mass distribution the moments of inertia of the spacecraft are proportional to the mass of the spacecraft. Thus, the attitude perturbations the spacecraft experiences are proportional to the reciprocal of the mass. In a similar fashion, the attitude perturbations are proportional to the reciprocal of the distance to the nucleus squared $\Delta(t)^{-2}$, because of the radial outflow approximation.

5. Discussion

The attitude perturbations simulated by our numerical model for the Giotto case are in the same order of magnitude as the measured perturbations (see Table 2). Hence, the numerical model is able to reproduce the measurements described by [4,27]. Because the measurements of Giotto are only one data point of an observation that is subject to large statistical fluctuations (see Figs. 1 and 2) we cannot draw any more precise conclusions from this comparison. The reproduction of those measurements does suggest however that the numerical model can provide relevant results. Further, it implies that the approximations and assumptions are appropriate when modelling the encounter with comet 1P/Halley by Giotto. However, the goodness of the approximations can be different when modelling Comet Interceptor. More specifically the approximation of the spacecraft as a cylinder with a homogeneous mass distribution is good in the case of Giotto, but might eventually be poor in the case of Comet Interceptor. In particular, larger structures like solar panel or antennas that could potentially increase the frontal area of the spacecraft significantly without adding a proportional amount of mass could lead to significantly smaller moments of inertia than estimated by using the assumption of a homogeneous mass distribution. Therefore, the assumptions need to be reevaluated once the basic spacecraft design is specified.

The exponents of the trendlines shown in Fig. 4 and listed in Table 4 give us an estimate of the proportionality of the attitude perturbations to the free parameters. The most crucial parameters are the encounter velocity v, the spacecraft radius R and the time interval

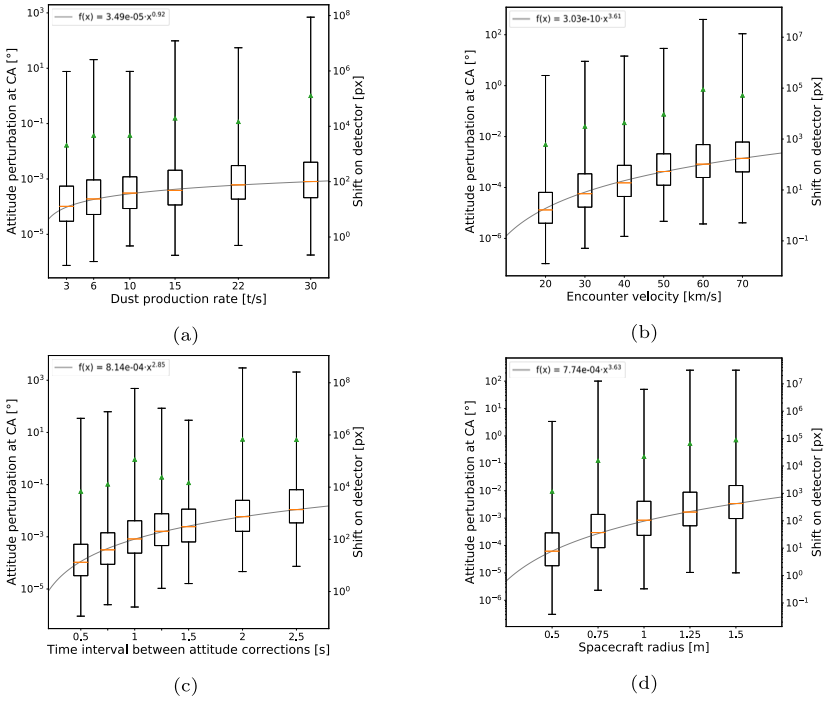

Fig. 4. Boxplots showing the attitude perturbations at closest approach in dependence of (a) dust production rate, (b) encounter velocity, (c) time interval between the attitude corrections and (d) spacecraft radius. The boxplots show minimum, 25th percentile, median, 75th percentile, mean (green triangle) and maximum. The trendlines are fitted to the medians based on a power law of the form $f(x) = a \cdot x^b$ using a least-squares fit. The input parameters are set as $\Delta T = 1$ s, $M = 500$ kg, $Q_d = 30000$ kg/s, $H = 1.5$ m, $\Delta_{CA} = 1000$ km, $v = 60$ km/s, $R = 1$ m.

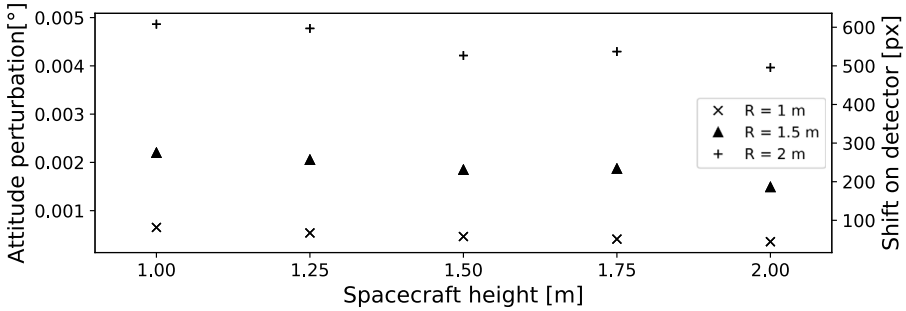

Fig. 5. Median attitude perturbation at closest approach for different combinations of the spacecraft radius and height. The other input parameters are set as $\Delta T = 1$ s, $M = 500$ kg, $Q_d = 30000$ kg/s, $\Delta_{CA} = 1000$ km, $v = 60$ km/s.

between attitude corrections ΔT. There are two different approaches to rank the importance of the parameters. The first approach is to look at the exponent of the trendlines whereas the second approach is to look at the range of attitude perturbations inside the chosen range of the parameter. With the first approach the spacecraft radius and the encounter velocity are considered the most crucial followed by the interval between attitude correction. However, with the second approach the order is reversed with the time interval between attitude corrections considered to be the most crucial parameter, followed by encounter velocity and spacecraft radius.

The attitude perturbations $\Delta\Phi$ are roughly proportional to the encounter velocity cubed (to be precise: $\Delta\Phi \propto v^{3.61}$) as shown in Fig. 4(b). Hence, the difference between encountering an object with a prograde orbit ($v \approx 30$ km/s) or with a retrograde orbit ($v \approx 60$ km/s) is about an order of magnitude in terms of the experienced attitude perturbations. This is due to the difference in the momentum of the dust particles, the difference in the momentum of recoil particles (see momentum enhancement factor Eq. (6)) and the difference in the number of dust particle impacts in a given time interval. More precisely, the difference in the total angular momentum change is proportional to $v^{2.31}$. But, for a higher encounter velocity the spacecraft experiences the angular momentum changes in a smaller time span. Thus, the attitude perturbations are larger unless the GNC is acting on a shorter time scale. As seen in Fig. 4(d), the proportionality of the attitude perturbations to the spacecraft radius is $\Delta\Phi \propto \mathrm{R}^{3.61}$ for a given height of 1.5 m. There is a stronger dependence on the radius for larger spacecraft heights and a weaker dependence for smaller heights. The relationship between attitude perturbations and time interval between attitude corrections is $\Delta\Phi \propto \Delta T^{2.85}$. However, there are many more free parameters associated with the GNC than modelled in this idealized case. Therefore, the implementation of the GNC is possibly more crucial than the encounter velocity or the radius of the spacecraft.

One of the less influential input parameters is the dust production rate. The attitude perturbations are proportional to $Q_d{}^{0.92}$. This can be explained by the fact that the local dust density is proportional to Q_d/v_d and the bulk dust velocity is faster for higher production rates. The least important input parameter is the height of the spacecraft, because as seen in Fig. 5 the effect of the height is negligible in comparison to the radius of the spacecraft. However, although the attitude perturbations are only slightly lower for a higher spacecraft

when keeping the radius constant, there is a larger effect when keeping the volume of the spacecraft constant.

6. Conclusion

Our numerical model is able to reproduce the attitude perturbations experienced by Giotto during its encounter with comet 1P/Halley. Our analysis shows that the most crucial parameters are the encounter velocity, the time interval between attitude correction and the spacecraft radius as might be predicted, but here we show clearly the dependencies on those parameters. The attitude perturbations experienced when encountering an object with a retrograde orbit are larger by an order of magnitude compared to the encounter with a prograde object. Frequent attitude corrections can lower the attitude perturbations by orders of magnitude. The large influence of the spacecraft radius shows that in general spacecrafts with smaller frontal areas are desirable for cometary encounter missions.

Based on our numerical model we believe that there is a high risk of losing a few images due to the impact of large dust particles. This is clearly demonstrated in Fig. 2(a), which shows several large dust particle impacts that would have shifted the target object mostly or completely out of the FOV. To ensure that CoCa is able to acquire images throughout the encounter the GNC needs to be able to correct for a few discrete impacts that can cause potentially very large attitude perturbations on the order of a few degrees (see Figs. 2(a) and 4). Additionally, the total $\Delta\omega$ needed to correct for all the attitude perturbations during the encounter is expected to be about 1-10°/s (see Fig. 3).

Apart from attitude perturbations of the spacecraft this model does not consider other sources of pointing errors caused by dust particle impacts such as vibrations. To ensure that the pointing errors are within the science requirements of the mission this should be modelled in a further study.

This work shows that the GNC needs to act on a time scale of a few seconds.

Declaration of competing interest

The authors declare that they have no known competing financial interests or personal relationships that could have appeared to influence the work reported in this paper.

Acknowledgements

This work has been carried out within the framework of the National Centre of Competence in Research PlanetS supported by the Swiss National Science Foundation. The authors acknowledge the financial support of the SNSF, Switzerland.

Appendix

Algorithm 1 Basic structure of the code

```
reset all the parameters
for i < number of iterations do
  for t < end time do
    calculate local dust number density
    generate the impacts in the current time step for each size bin
    calculate the resulting changes in velocity and angular velocity
    v(t) ← v(t − 1) + Δv
    ω(t) ← ω(t − 1) + Δω
    position(t) ← position(t − 1) + v(t) · Δt
    attitude(t) ← attitude(t − 1) + ω(t) · Δt
  end for
end for
```

References

[1] C. Snodgrass, G.H. Jones, The European Space Agency's Comet Interceptor lies in wait, Nat. Commun. 10 (1) (2019) 5418, http://dx.doi.org/10.1038/s41467-019-13470-1.

[2] M.E. Schwamb, M.M. Knight, G.H. Jones, C. Snodgrass, L. Bucci, J.M. Sánchez Pérez, N. Skuppin, Potential backup targets for comet interceptor, Res. Notes AAS 4 (2) (2020) 21, http://dx.doi.org/10.3847/2515-5172/ab7300.

[3] R. Reinhard, Giotto mission, in: Encyclopedia of Planetary Science, Springer Netherlands, Dordrecht, 1997, pp. 274–279, http://dx.doi.org/10.1007/1-4020-4520-4_1560.

[4] W. Curdt, H.U. Keller, Large dust particles along the Giotto trajectory, Icarus 86 (1) (1990) 305–313, http://dx.doi.org/10.1016/0019-1035(90)90220-4, http://www.sciencedirect.com/science/article/pii/0019103590902204.

[5] P. Edenhofer, M.K. Bird, J.P. Brenkle, H. Buschert, E.R. Kursinki, N.A. Mottinger, H. Porsche, C.T. Stelzried, H. Volland, Dust distribution of Comet p/ Halley's inner coma determined from the giotta radio science experiment, Astron. Astrophys. 187 (1987) 712.

[6] V. Preda, A. Hyslop, S. Bennani, Optimal science-time reorientation policy for the Comet Interceptor flyby via sequential convex programming, CEAS Space J. 14 (1) (2022) 173–186, http://dx.doi.org/10.1007/s12567-021-00368-2.

[7] N.N. Smirnov, A.B. Kiselev, K.A. Kondratyev, S.N. Zolkin, Impact of debris particles on space structures modeling, Acta Astronaut. 67 (3) (2010) 333–343, http://dx.doi.org/10.1016/j.actaastro.2010.03.003, https://www.sciencedirect.com/science/article/pii/S0094576510000834.

[8] M.V. Silnikov, I.V. Guk, A.F. Nechunaev, N.N. Smirnov, Numerical simulation of hypervelocity impact problem for spacecraft shielding elements, Acta Astronaut. 150 (2018) 56–62, http://dx.doi.org/10.1016/j.actaastro.2017.08.030, https://www.sciencedirect.com/science/article/pii/S0094576517311888.

[9] N.N. Smirnov, A.B. Kiselev, P.P. Zakharov, Numerical simulation of the hypervelocity impact of the ball and the spherical containment in three-material statement, Acta Astronaut. 171 (2020) 215–224, http://dx.doi.org/10.1016/j.actaastro.2020.03.010, https://www.sciencedirect.com/science/article/pii/S0094576520301387.

[10] M.K. Wallis, Comet Halley's dust drag perturbing the Giotto spacecraft, Earth Moon Planets 30 (1) (1984) 31–37, http://dx.doi.org/10.1007/BF00118088.

[11] N. Thomas, H.U. Keller, Interpretation of the inner coma observations of comet P/Halley by the Halley multicolour camera, Ann. Geophys. Atmos. Hydrospheres Space Sci. 8 (2) (1990) 147–166, http://inis.iaea.org/search/search.aspx?orig_q=RN:21073633.

[12] S.-B. Gerig, R. Marschall, N. Thomas, I. Bertini, D. Bodewits, B. Davidsson, M. Fulle, W.-H. Ip, H.U. Keller, M. Küppers, F. Preusker, F. Scholten, C.C. Su, I. Toth, C. Tubiana, J.-S. Wu, H. Sierks, C. Barbieri, P.L. Lamy, D. Rodrigo, H. Rickman, J. Agarwal, M.A. Barucci, J.-L. Bertaux, G. Cremonese, V. Da Deppo, S. Debei, M. De Cecco, J. Deller, S. Fornasier, O. Groussin, P.J. Gutierrez, C. Güttler, S.F. Hviid, L. Jorda, J. Knollenberg, J.-R. Kramm, E. Kührt, L.M. Lara, M. Lazzarin, J.J. Lopez Moreno, F. Marzari, S. Mottola, G. Naletto, N. Oklay, J.-B. Vincent, On deviations from free-radial outflow in the inner coma of comet 67P/Churyumov-Gerasimenko, Icarus 311 (2018) 1–22, http://dx.doi.org/10.1016/j.icarus.2018.03.010.

[13] N. Thomas, An Introduction to Comets - Post-Rosetta Perspectives, Springer, 2020, http://dx.doi.org/10.1007/978-3-030-50574-5.

[14] J.A.M. McDonnell, G.C. Evans, S.T. Evans, W.M. Alexander, W.M. Burton, J.G. Firth, E. Bussoletti, R.J.L. Grard, M.S. Hanner, Z. Sekanina, T.J. Stevenson, R.F. Turner, U. Weishaupt, M.K. Wallis, J.C. Zarnecki, The dust distribution within the inner coma of comet P/Halley 1982i - Encounter by Giotto's impact detectors, Astron. Astrophys. 187 (1-2) (1987) 719–741.

[15] J.A.M. McDonnell, P.L. Lamy, G.S. Pankiewicz, Physical properties of cometary dust, Int. Astron. Union Colloquium 116 (2) (1991) 1043–1073, http://dx.doi.org/10.1017/S0252921100012811.

[16] J. McDonnell, J. Kissel, E. Grün, R. Grard, Y. Langevin, R. Olearczyk, C. Perry, John Zarnecki, Giotto's Dust Impact Detection System (DIDSY) and Particulate Impact Analyzer (PIA): Interim assessment of the dust distribution and properties within the coma 250 (1986) 25–38.

[17] K. Richter, Werner Curdt, H. Keller, Velocity of individual large dust particles ejected from comet p/halley, Astron. Astrophys. 250 (1991) 548–555.

[18] R. Marschall, C.C. Su, Y. Liao, N. Thomas, K. Altwegg, H. Sierks, W.-H. Ip, H.U. Keller, Modelling observations of the inner gas and dust coma of comet 67P/Churyumov-Gerasimenko using ROSINA/COPS and OSIRIS data: First results, Astron. Astrophys. 589 (2016) A90.

[19] R. Marschall, S. Mottola, C.C. Su, Y. Liao, M. Rubin, J.S. Wu, N. Thomas, K. Altwegg, H. Sierks, W.-H. Ip, H.U. Keller, J. Knollenberg, E. Kührt, I.L. Lai, Y. Skorov, L. Jorda, F. Preusker, F. Scholten, J.-B. Vincent, Osiris Team, Rosina Team, Cliffs versus plains: Can ROSINA/COPS and OSIRIS data of comet 67P/Churyumov-Gerasimenko in autumn 2014 constrain inhomogeneous outgassing? Astron. Astrophys. 605 (2017) A112, http://dx.doi.org/10.1051/0004-6361/201730849.

[20] R. Marschall, L. Rezac, D. Kappel, C.C. Su, S.-B. Gerig, M. Rubin, O. Pinzón-Rodrí guez, D. Marshall, Y. Liao, C. Herny, G. Arnold, C. Christou, S.K. Dadzie, O. Groussin, P. Hartogh, L. Jorda, E. Kührt, S. Mottola, O. Mousis, F. Preusker, F. Scholten, P. Theologou, J.-S. Wu, K. Altwegg, R. Rodrigo, N. Thomas, A comparison of multiple rosetta data sets and 3D model calculations of 67P/Churyumov-Gerasimenko coma around equinox (May 2015), Icarus 328 (2019) 104–126, http://dx.doi.org/10.1016/j.icarus.2019.02.008, http://www.sciencedirect.com/science/article/pii/S0019103518305700.

[21] R. Marschall, J. Markkanen, S.-B. Gerig, O. Pinzón-Rodríguez, N. Thomas, Jong-Shinn Wu, The dust-to-gas ratio, size distribution, and dust fall-back fraction of comet 67P/Churyumov-Gerasimenko: Inferences from linking the optical and dynamical properties of the inner comae, Front. Phys. 8 (2020) 227, http://dx.doi.org/10.3389/fphy.2020.00227.

[22] S.-B. Gerig, O. Pinzón-Rodríguez, R. Marschall, J.-S. Wu, N. Thomas, Dayside-to-nightside dust coma brightness asymmetry and its implications for nightside activity at Comet 67P/Churyumov-Gerasimenko, Icarus 351 (2020) http://dx.doi.org/10.1016/j.icarus.2020.113968.

[23] T. Gombosi, Thomas Cravens, A. Nagy, Time-dependent dusty gasdynamical flow near cometary nuclei, Astrophys. J. 293 (1985) http://dx.doi.org/10.1086/163240.

[24] J.-F. Crifo, G.A. Loukianov, A.V. Rodionov, V.V. Zakharov, Direct Monte Carlo and multifluid modeling of the circumnuclear dust coma: Spherical grain dynamics revisited, Icarus 176 (1) (2005) 192–219, http://dx.doi.org/10.1016/j.icarus.2005.01.003, https://www.sciencedirect.com/science/article/pii/S0019103505000060.

[25] M. Pätzold, T.P. Andert, M. Hahn, J.-P. Barriot, S.W. Asmar, B. Häusler, M.K. Bird, S. Tellmann, J. Oschlisniok, K. Peter, The Nucleus of comet 67P/Churyumov–Gerasimenko–Part I: The global view–nucleus mass, mass-loss, porosity, and implications, Mon. Not. R. Astron. Soc. 483 (2) (2018) 2337–2346, http://dx.doi.org/10.1093/mnras/sty3171.

[26] J.A.M. McDonnell, Momentum enhancement in hypervelocity impacts: Parameters for space debris and meteoroid perturbations, in: 5th Cranfield DCSSS Conference, 2002.

[27] P. Edenhofer, H. Buschert, H. Porsche, M.K. Bird, H. Volland, J.P. Brenkle, E.R. Kursinsky, N.A. Mottinger, C.T. Stelzried, Dust distribution of Comet Halley from the Giotto radio science experiment, in: B. Battrick, E.J. Rolfe, R. Reinhard (Eds.), ESLAB Symposium on the Exploration of Halley's Comet, in: ESA Special Publication, 250, 1986, pp. 215–218.

[28] R. Reinhard, The Giotto encounter with comet Halley, Nature 321 (6067) (1986) 313–318, http://dx.doi.org/10.1038/321313a0.

[29] N. Thomas, H.U. Keller, Comet P/Halley's dust production rate at Giotto encounter derived from Halley Multicolour Camera observations, Astron. Astrophys. 249 (1) (1991) 258–268.

[30] N. Thomas, G. Cremonese, R. Ziethe, M. Gerber, M. Brändli, G. Bruno, M. Erismann, L. Gambicorti, T. Gerber, K. Ghose, M. Gruber, P. Gubler, H. Mischler, J. Jost, D. Piazza, A. Pommerol, M. Rieder, V. Roloff, A. Servonet, W. Trottmann, T. Uthaicharoenpong, C. Zimmermann, D. Vernani, M. Johnson, E. Pelò, T. Weigel, J. Viertl, N. De Roux, P. Lochmatter, G. Sutter, A. Casciello, T. Hausner, I. Ficai Veltroni, V. Da Deppo, P. Orleanski, W. Nowosielski, T. Zawistowski, S. Szalai, B. Sodor, S. Tulyakov, G. Troznai, M. Banaskiewicz, J.C. Bridges, S. Byrne, S. Debei, M.R. El-Maarry, E. Hauber, C.J. Hansen, A. Ivanov, L. Keszthelyi, R. Kirk, R. Kuzmin, N. Mangold, L. Marinangeli, W.J. Markiewicz, M. Massironi, A.S. McEwen, C. Okubo, L.L. Tornabene, P. Wajer, J.J. Wray, The colour and stereo surface imaging system (CaSSIS) for the ExoMars trace gas orbiter, Space Sci. Rev. 212 (3) (2017) 1897–1944, http://dx.doi.org/10.1007/s11214-017-0421-1.